



Stony Brook **University**



Coherent Diffractive Dijet Production in Deep Inelastic Scattering and Dipole Orientation

Farid Salazar

Stony Brook University. Brookhaven National Laboratory

Advisor: Bjoern Schenke (BNL)

The Myriad Colorful Ways of Understanding Extreme QCD Matter

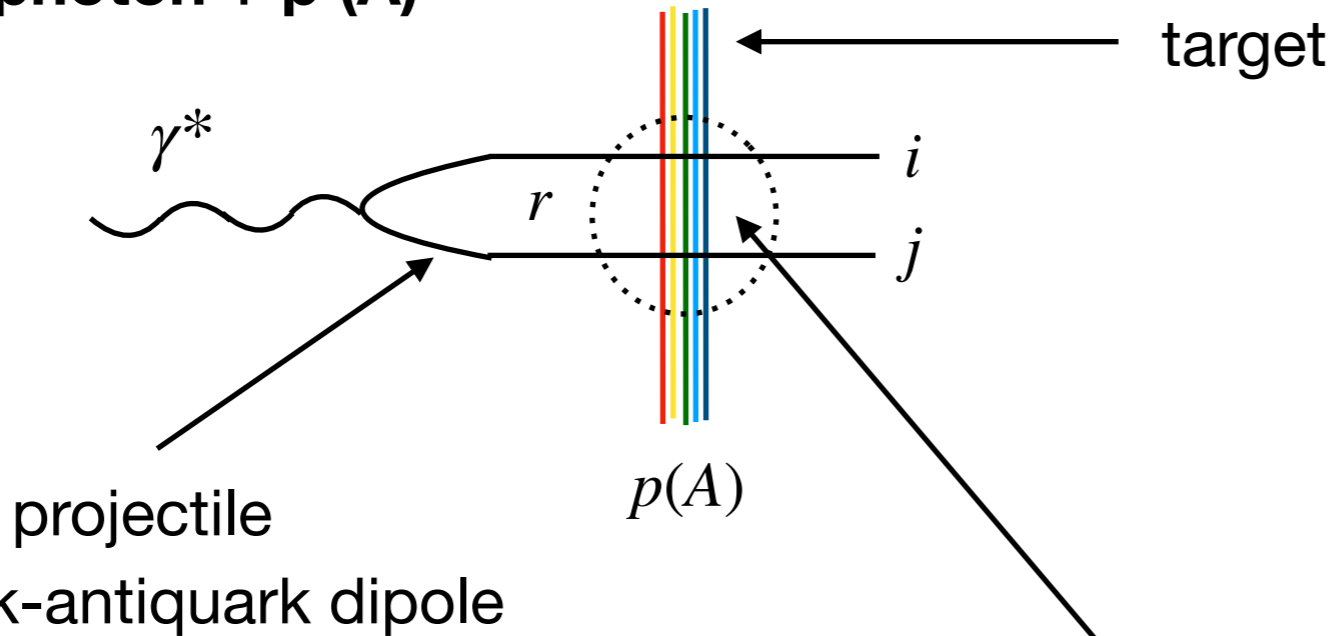
April 5th, 2019.

Outline

- High energy scattering in QCD
 - Target, projectile and the scattering
 - From amplitude to cross section
- Coherent diffractive dijet
 - Target geometry, dipole spatial correlations and cross section momentum correlations
 - Numerical approach
 - Semi-analytic approach
 - Conclusions/extensions

Target, projectile and the scattering amplitude

virtual photon + p (A)



Strong classical fields

$$A^{\mu,a} = \delta^{\mu,+} \alpha(\mathbf{x}, x^-)$$

$$\nabla_{\mathbf{x}}^2 \alpha^a(\mathbf{x}, x^-) = -\rho^a(\mathbf{x}, x^-)$$

small-x (fields)

large-x (sources)

scattering

dipole eikonal scattering from strong color fields

$$S_{ij}(\mathbf{x}, \mathbf{y}) = [V(\mathbf{x})V^\dagger(\mathbf{y})]_{ij}$$

$$V(\mathbf{x}) = P e^{-ig \int dz^- T^a \alpha^a(z^-, \mathbf{x})}$$

$$\Psi_L^{\gamma^* \rightarrow q\bar{q}}(\mathbf{r}) = \frac{eZ_f}{2\pi} z_0^{3/2} z_1^{3/2} 2Q(1 - \delta_{\sigma_0\sigma_1}) K_0(\varepsilon_f r)$$

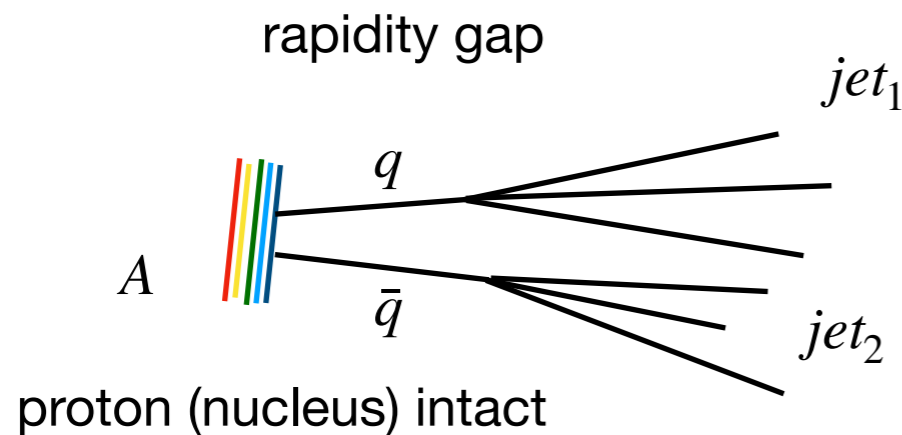
$$\Psi_{T\lambda}^{\gamma^* \rightarrow q\bar{q}}(\mathbf{r}) = \frac{eZ_f}{2\pi} z_0 z_1 \left[\delta_{\sigma_0\sigma_1} \frac{m_f}{\sqrt{2}} (1 + \sigma_0 \lambda) K_0(\varepsilon_f r) + \delta_{\sigma_0-\sigma_1} (z_1 - z_0 - \sigma_0 \lambda) i \varepsilon_f \frac{\boldsymbol{\epsilon}_\lambda \cdot \mathbf{r}}{r} K_1(\varepsilon_f r) \right]$$

$$\varepsilon_f^2 = z_0 z_1 Q^2 + m_f^2$$

From amplitude to cross section

$$\mathcal{M}(\mathbf{x}_1, \mathbf{x}_2) = \Psi(|\mathbf{x}_1 - \mathbf{x}_2|) [1_c - V(\mathbf{x}_1)V^\dagger(\mathbf{x}_2)] \quad \tilde{\mathcal{M}}(\mathbf{p}_1, \mathbf{p}_2) = \int d^2\mathbf{x}_1 \int d^2\mathbf{x}_2 e^{i\mathbf{x}_1 \cdot \mathbf{p}_1} e^{i\mathbf{x}_2 \cdot \mathbf{p}_2} \mathcal{M}(\mathbf{x}_1, \mathbf{x}_2)$$

Coherent diffractive dijet



$$\frac{d\sigma^{coh\ diff}}{d\Omega} \sim \left| \langle \text{tr} \mathcal{M}(\mathbf{p}_1, \mathbf{p}_2) \rangle \right|^2$$

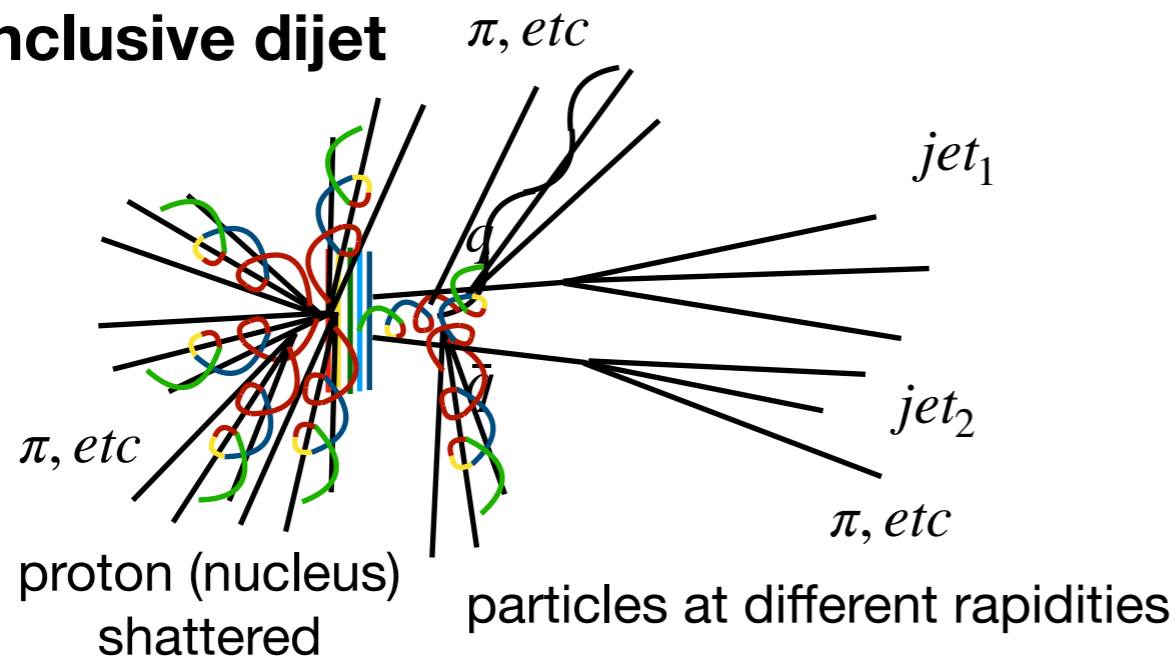
↑

scattered dipole in color singlet

↑

prescription for coherent process

Inclusive dijet



$$\frac{d\sigma^{inclusive}}{d\Omega} \sim \text{tr} \left\langle \left| \mathcal{M}(\mathbf{p}_1, \mathbf{p}_2) \right|^2 \right\rangle$$

↑

sum over color in final states

↑

prescription for inclusive process

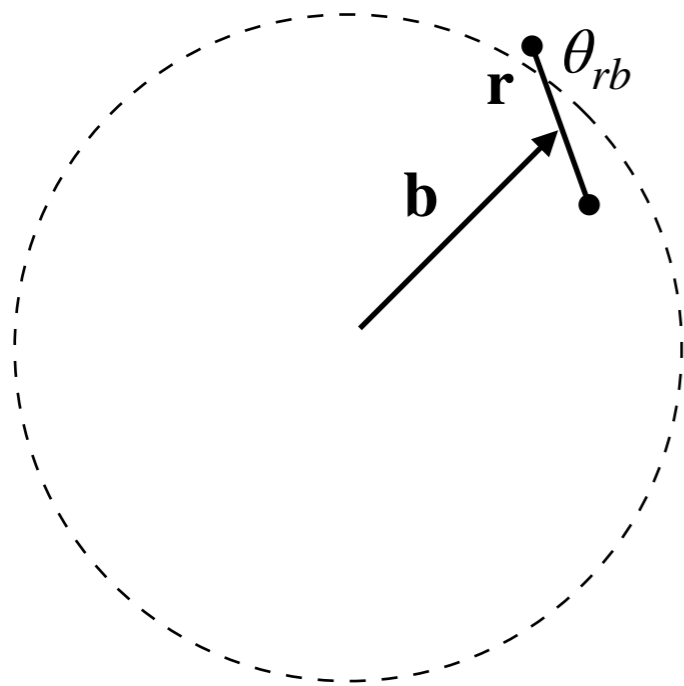
Target geometry, dipole spatial correlations and cross section momentum correlations

$$p_0^+ p_1^+ \frac{d\sigma^{\text{coh diff}}}{dp_0^+ dp_1^+ d^2\mathbf{P} d^2\mathbf{\Delta}} = \frac{\delta(q^+ - p_0^+ - p_1^+)}{2q^+(2\pi)^5} \left| \int d^2\mathbf{r} d^2\mathbf{b} e^{-i\mathbf{P}\cdot\mathbf{r}} e^{-i\mathbf{\Delta}\cdot\mathbf{b}} \Psi(\mathbf{r}) D(\mathbf{r}, \mathbf{b}) \right|^2$$

$$D(\mathbf{r}, \mathbf{b}) = \left[1 - \frac{1}{N_c} \left\langle \text{tr} \left(V(\mathbf{b} + \frac{\mathbf{r}}{2}) V^\dagger(\mathbf{b} - \frac{\mathbf{r}}{2}) \right) \right\rangle \right]$$

$$\begin{aligned} \mathbf{r} = \mathbf{x}_1 - \mathbf{x}_2 & \longleftrightarrow \mathbf{P} = \frac{1}{2} (\mathbf{p}_1 - \mathbf{p}_2) \\ \mathbf{b} = \frac{1}{2} (\mathbf{x}_1 + \mathbf{x}_2) & \longleftrightarrow \mathbf{\Delta} = \mathbf{p}_1 + \mathbf{p}_2 \end{aligned}$$

Fourier conjugates



Transverse view of target

Target geometry



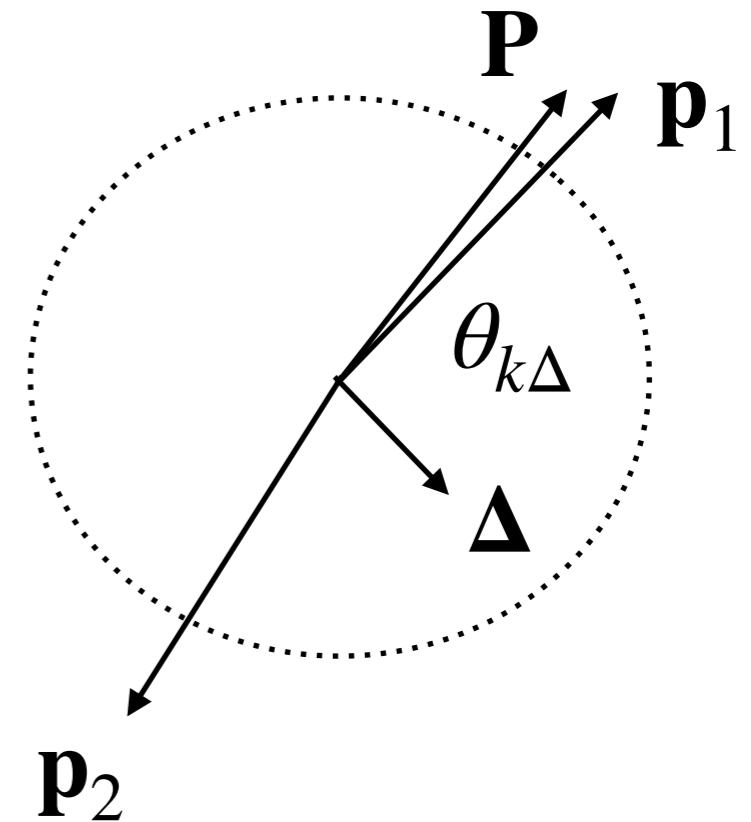
b dependence

θ_{rb} dependence
(dipole orientation)



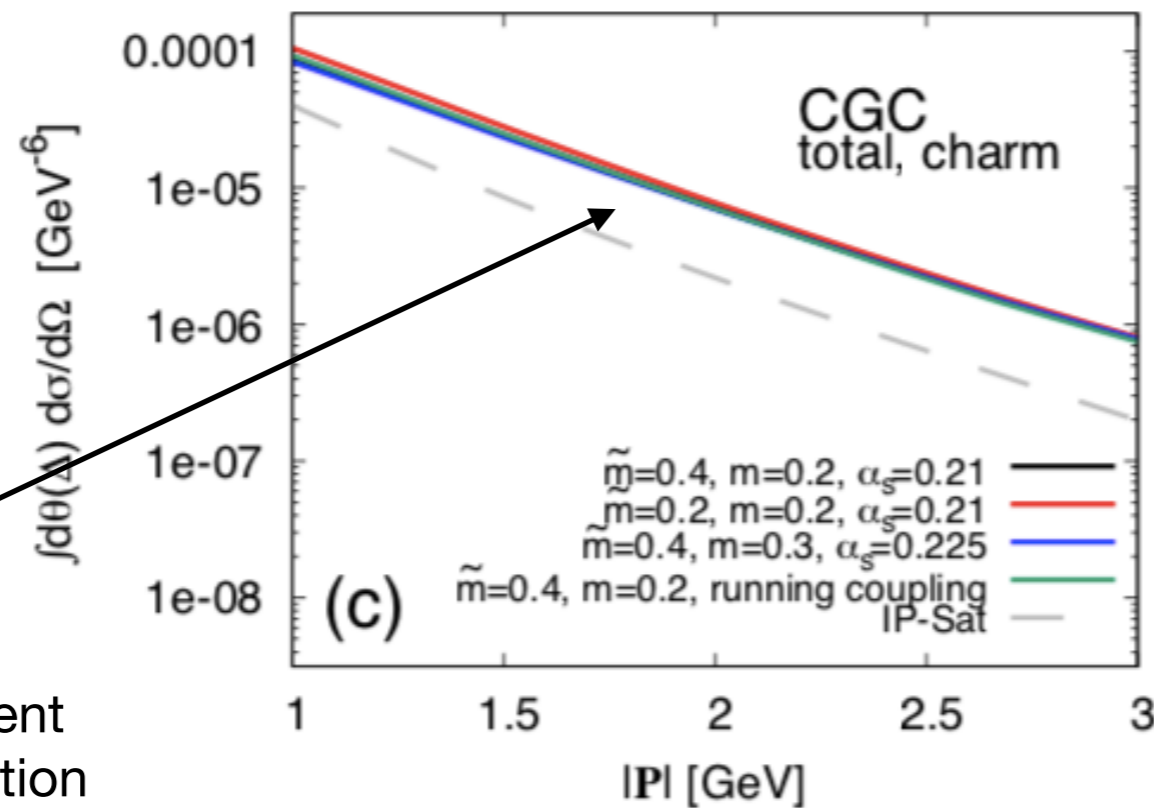
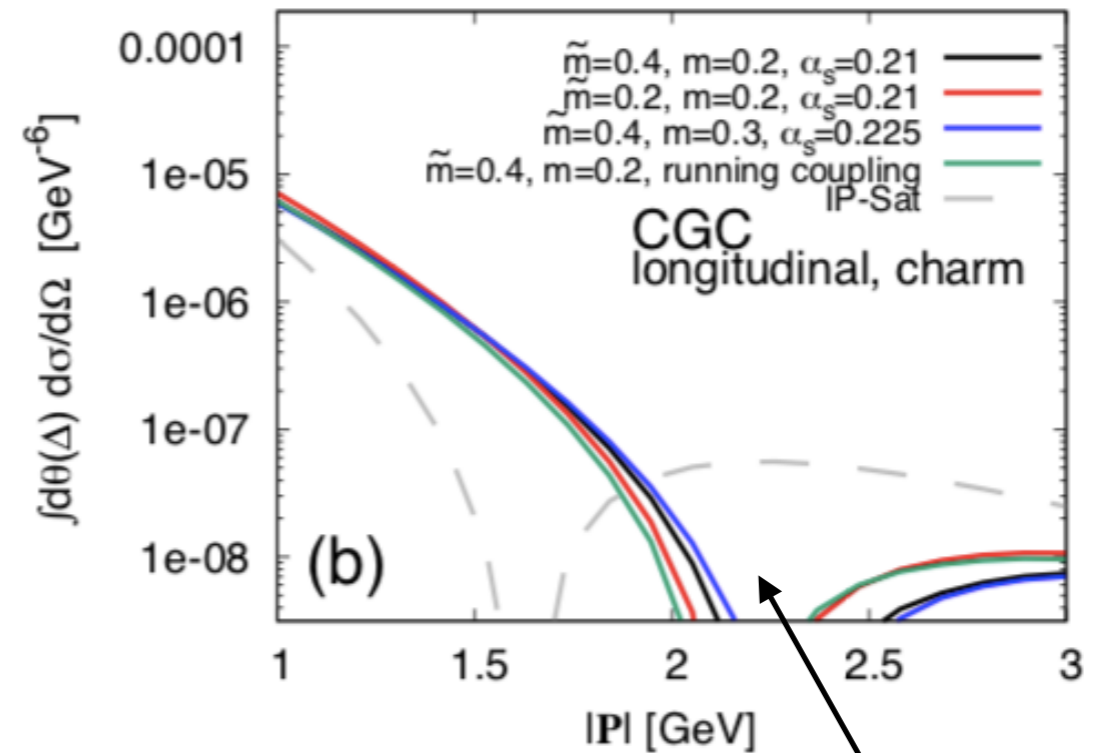
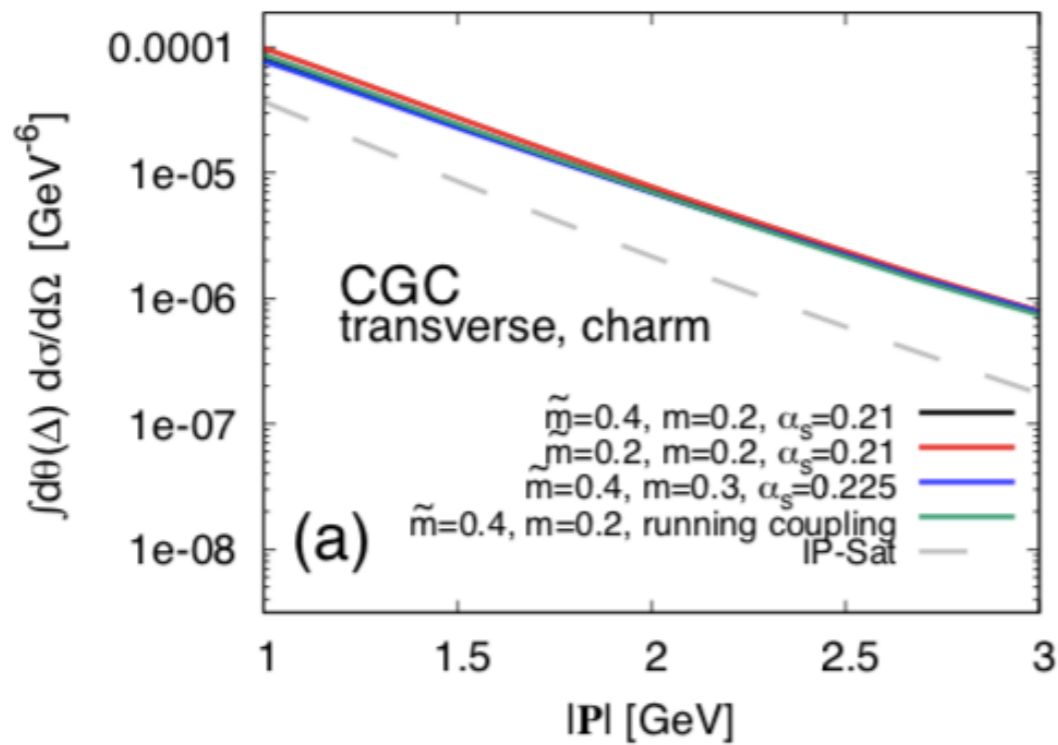
P dependence

$\theta_{P\Delta}$ dependence
(elliptic anisotropy)



$$\frac{d\sigma}{d\Omega}(\mathbf{P}, \mathbf{\Delta}) = \frac{d\sigma_0}{d\Omega}(P, \Delta) + 2 \frac{d\sigma_2}{d\Omega}(P, \Delta) \cos 2\theta_{P\Delta} + \dots$$

Numerical results: Differential Cross section (Proton)

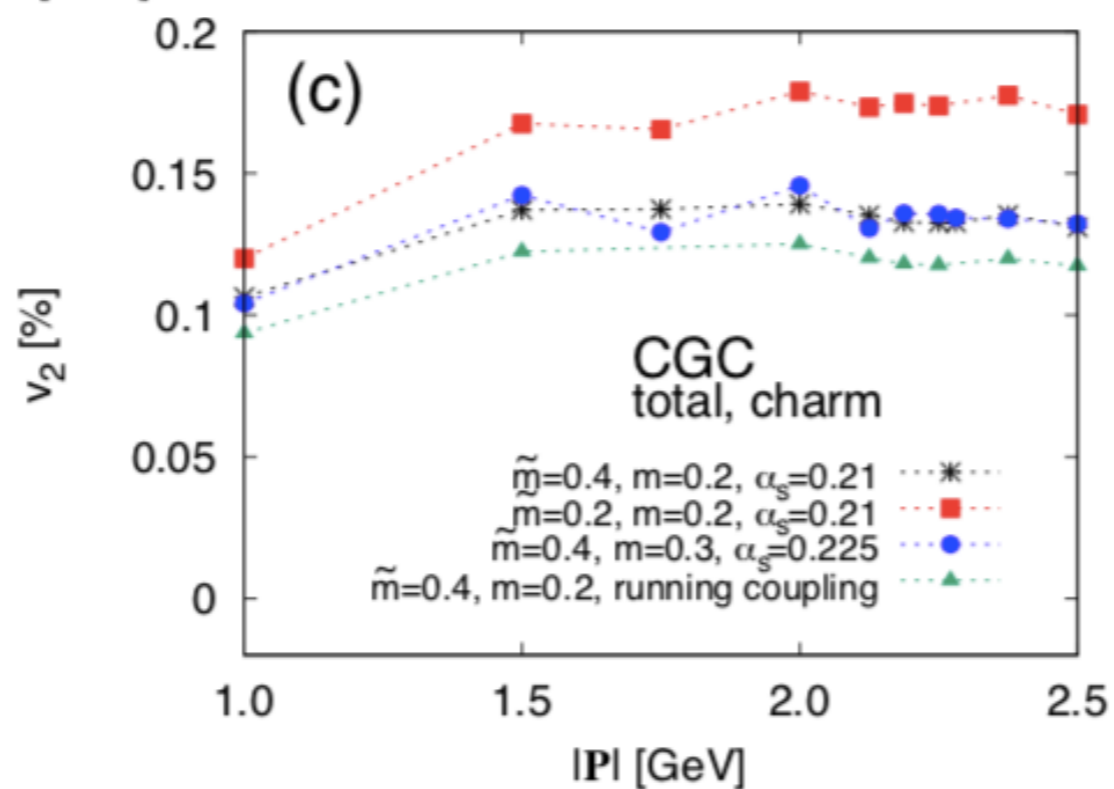
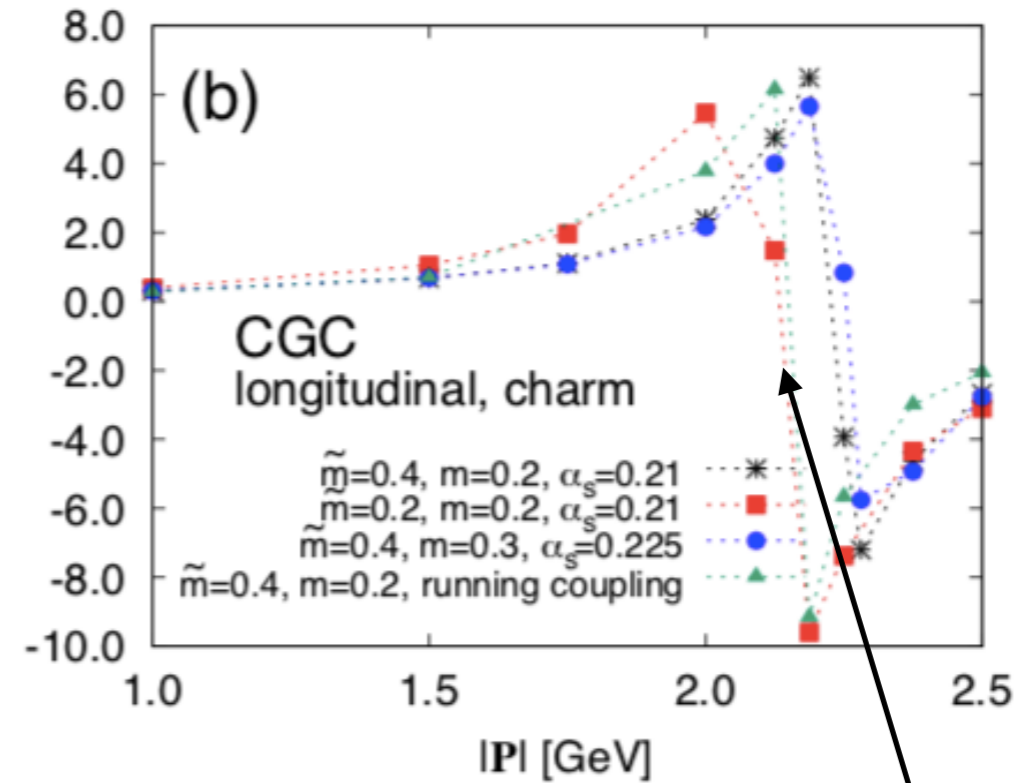
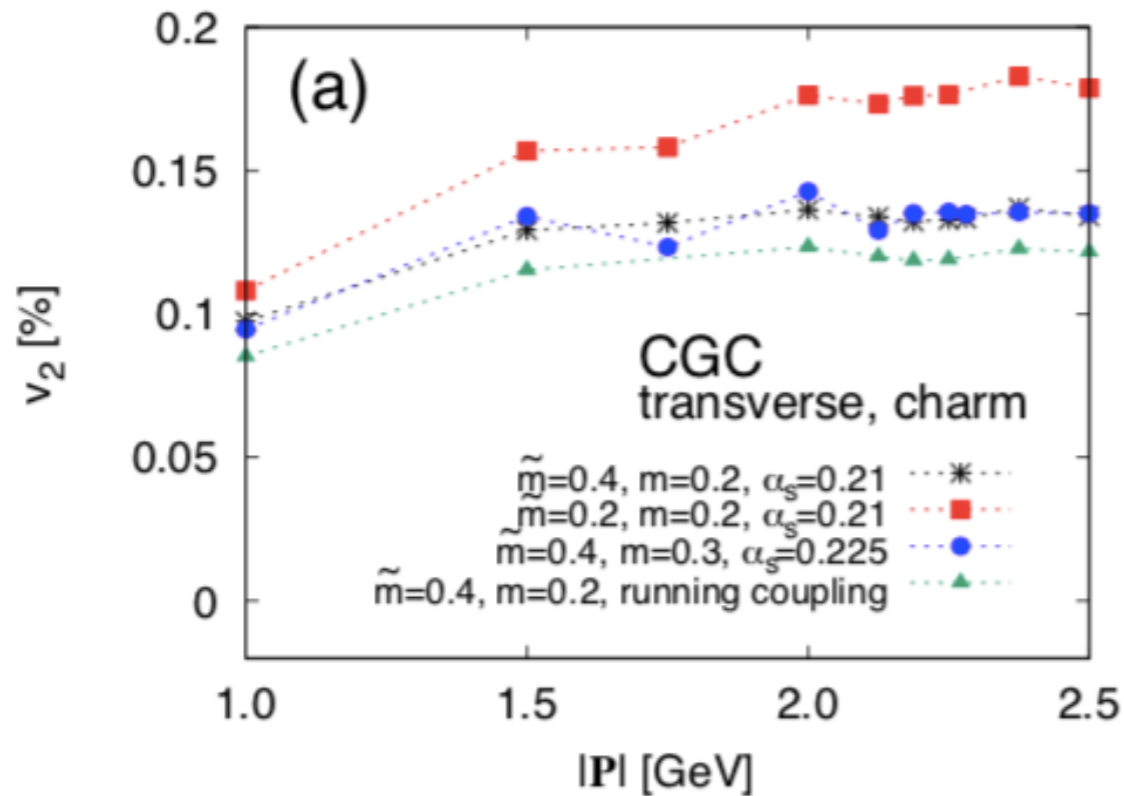


no dip in P
transverse component
dominates cross section

dip in P arising from
projectile wave function
and dipole amplitude r
dependence

Diffractive dijet production and Wigner
distributions from the color glass condensate
Mantysaari, Mueller, Schenke. arxiv:
1902.05087

Numerical results: Relative Elliptic Anisotropy (Proton)



change in sign of elliptic anisotropy at the location of dip

Diffractive dijet production and Wigner distributions from the color glass condensate
 Mantysaari, Mueller, Schenke. arxiv: 1902.05087

Semi-analytic approach to coherent diffractive dijet

Classical Computation of Elliptic Flow at Large Transverse Momentum.
Teaney, Venugopalan. Phys.Lett.B539:53-58 (2002)

Key ingredients for semi-analytic approach

Elliptic flow from color-dipole orientation in pp and pA collisions
Iancu, Rezaeian. PhysRevD.95.094003 (2017)

- Dipole amplitude for extended MV with impact parameter:

$$\langle \rho^a(x^-, \mathbf{x}) \rho^b(y^-, \mathbf{y}) \rangle = g^2 \mu^2 \delta^{(2)}(\mathbf{x} - \mathbf{y}) \delta(x^- - y^-) T(\mathbf{x})$$

$$\mathcal{N}_0(r, b) = \frac{1}{4} Q_s^2 r^2 \log \left(\frac{1}{m^2 r^2} + e \right) T(b) + \dots \quad \mathcal{N}_2(r, b) = \frac{1}{4} Q_s^2 r^2 \frac{1}{6m^2} \left[\frac{d^2}{db^2} - \frac{1}{b} \frac{1}{db} \right] T(b) + \dots$$

- One-to-one relation between harmonics of amplitude and harmonics of Fourier transform of amplitude.

$$D(\mathbf{r}, \mathbf{b}) = 1 - e^{-(\mathcal{N}_0(r, b) + \mathcal{N}_2(r, b) \cos 2\theta_{rb})}$$

$$D_0(r, b) = 1 - e^{-\mathcal{N}_0(r, b)} I_0(\mathcal{N}_2(r, b))$$

$$D_2(r, b) = e^{-\mathcal{N}_0(r, b)} I_1(\mathcal{N}_2(r, b))$$

$$\mathcal{M}(\mathbf{r}, \mathbf{b}) = \mathcal{M}_0(r, b) + 2\mathcal{M}_2(r, b) \cos 2\theta_{rb} + \dots$$

$$\tilde{\mathcal{M}}(\mathbf{P}, \mathbf{\Delta}) = \tilde{\mathcal{M}}_0(P, \Delta) + 2\tilde{\mathcal{M}}_2(P, \Delta) \cos 2\theta_{P\Delta} + \dots$$

$$\tilde{\mathcal{M}}_k(P, \Delta) = \int r dr b db J_k(Pr) J_k(\Delta b) \mathcal{M}_k(r, b)$$

Numerics vs Semi-analytics

$$\int d^2\mathbf{r} d^2\mathbf{b} e^{-i\mathbf{P}\cdot\mathbf{r}} e^{-i\mathbf{\Delta}\cdot\mathbf{b}} \Psi(\mathbf{r})D(\mathbf{r}, \mathbf{b})$$

MonteCarlo
integration

Sample ρ configurations.
Construct Wilson lines, then
dipole.
JIMWLK evolution.
Average over configurations.

$$\langle \rho^a(x^-, \mathbf{x}) \rho^b(y^-, \mathbf{y}) \rangle = g^2 \mu^2 \delta^{(2)}(\mathbf{x} - \mathbf{y}) \delta(x^- - y^-) T(\mathbf{x})$$

Limitations

- From the numerical approach it is difficult to understand analytic properties of cross section and elliptic anisotropy.
- Furthermore, due to oscillating behavior in Fourier transform computation expensive for large \mathbf{P} or $\mathbf{\Delta}$.

$$\tilde{F}_0(P, \Delta) = \int r dr b db J_0(Pr) J_0(\Delta b) K_0(\epsilon_f r) D_0(r, b)$$

$$\tilde{F}_2(P, \Delta) = \int r dr b db J_2(Pr) J_2(\Delta b) K_0(\epsilon_f r) D_2(r, b)$$

$$\tilde{G}_0(P, \Delta) = - \int r dr b db J_1(Pr) J_0(\Delta b) K_1(\epsilon_f r) D_0(r, b)$$

$$\tilde{G}_2(P, \Delta) = - \int r dr b db \left[\frac{J_3(Pr) - J_1(Pr)}{2} \right] J_2(\Delta b) K_1(\epsilon_f r) D_2(r, b)$$

$$\frac{d\sigma_{L,0}}{d\Omega} = \frac{8N_c \alpha_{EM}}{(2\pi)^6} z_0^3 z_1^3 Q^2 Z_f^2 |\tilde{F}_0|^2$$

$$\frac{d\sigma_{L,2}}{d\Omega} = \frac{8N_c \alpha_{EM}}{(2\pi)^6} z_0^3 z_1^3 Q^2 Z_f^2 \Re \left(2\tilde{F}_0 \tilde{F}_2^* \right)$$

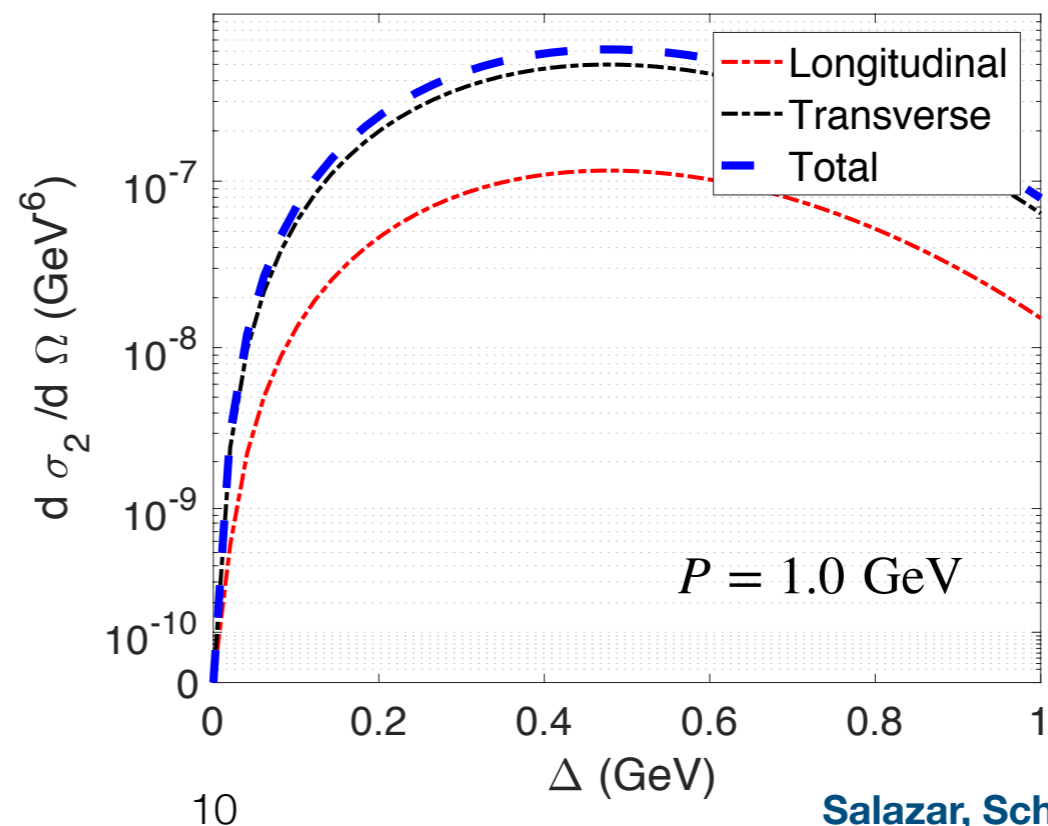
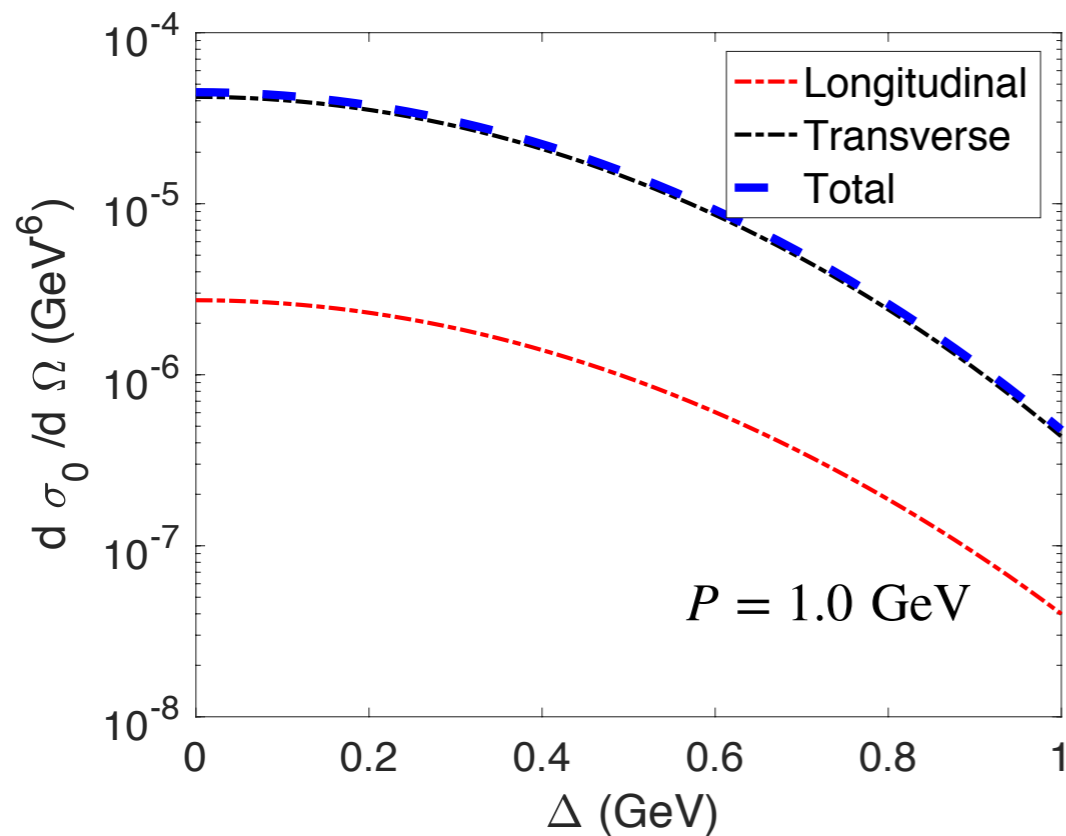
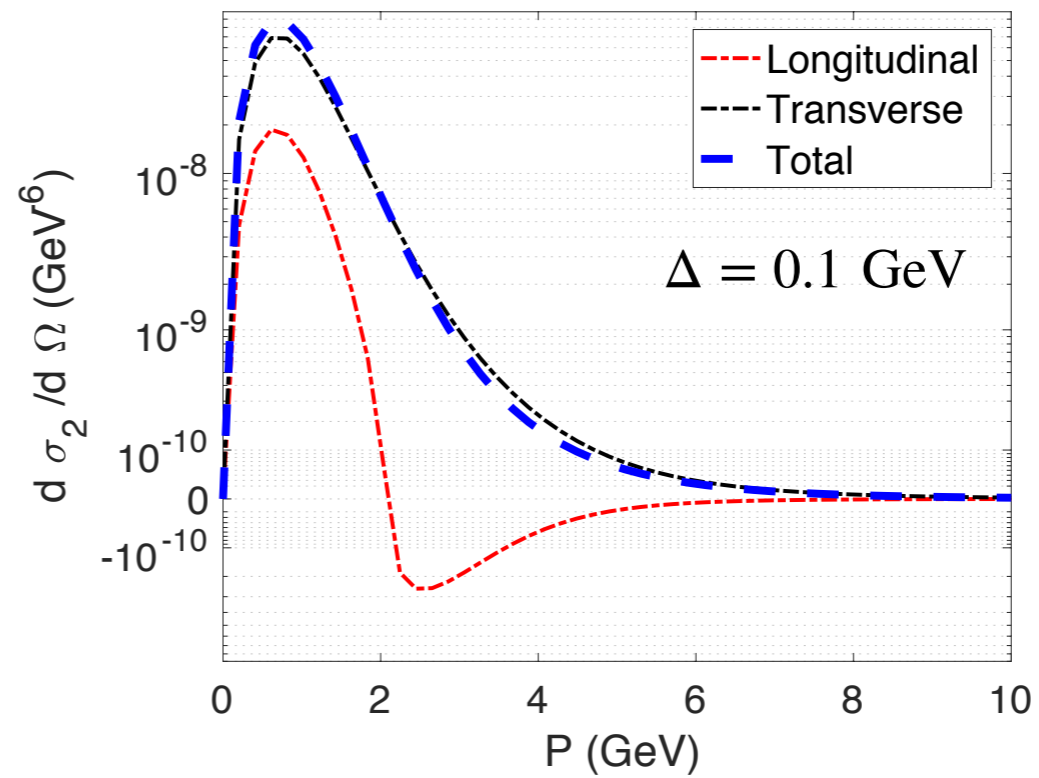
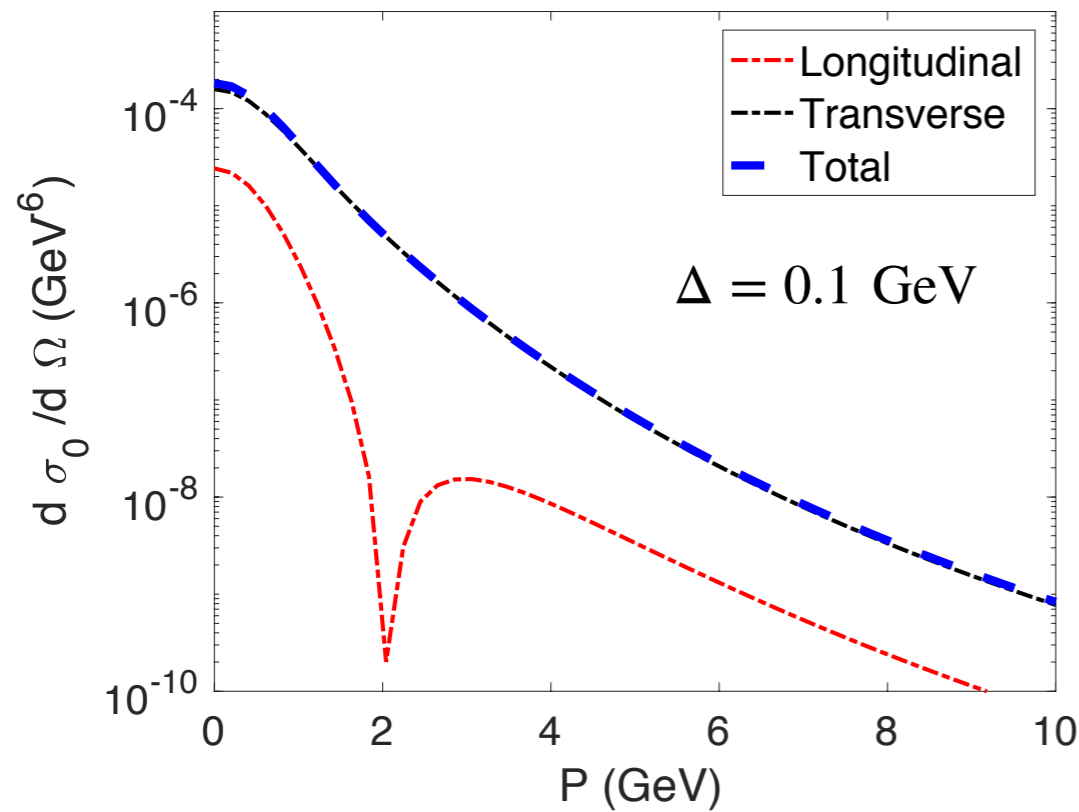
$$\frac{d\sigma_{T,0}}{d\Omega} = \frac{2N_c \alpha_{EM}}{(2\pi)^6} Z_f^2 z_0 z_1 \left\{ \epsilon_f^2 (z_0^2 + z_1^2) |\tilde{G}_0|^2 + m_f^2 |\tilde{F}_0|^2 \right\}$$

$$\frac{d\sigma_{T,2}}{d\Omega} = \frac{2N_c \alpha_{EM}}{(2\pi)^6} Z_f^2 z_0 z_1 \left\{ \epsilon_f^2 (z_0^2 + z_1^2) \Re \left(2\tilde{G}_0 \tilde{G}_2^* \right) + m_f^2 \Re \left(2\tilde{F}_0 \tilde{F}_2^* \right) \right\}$$

Limitations

- Only includes Gaussian correlations of sources.
- Does not account for growth of the proton, and possibly change of gradients.

Semi-analytic results: Cross section and Elliptic (Proton)



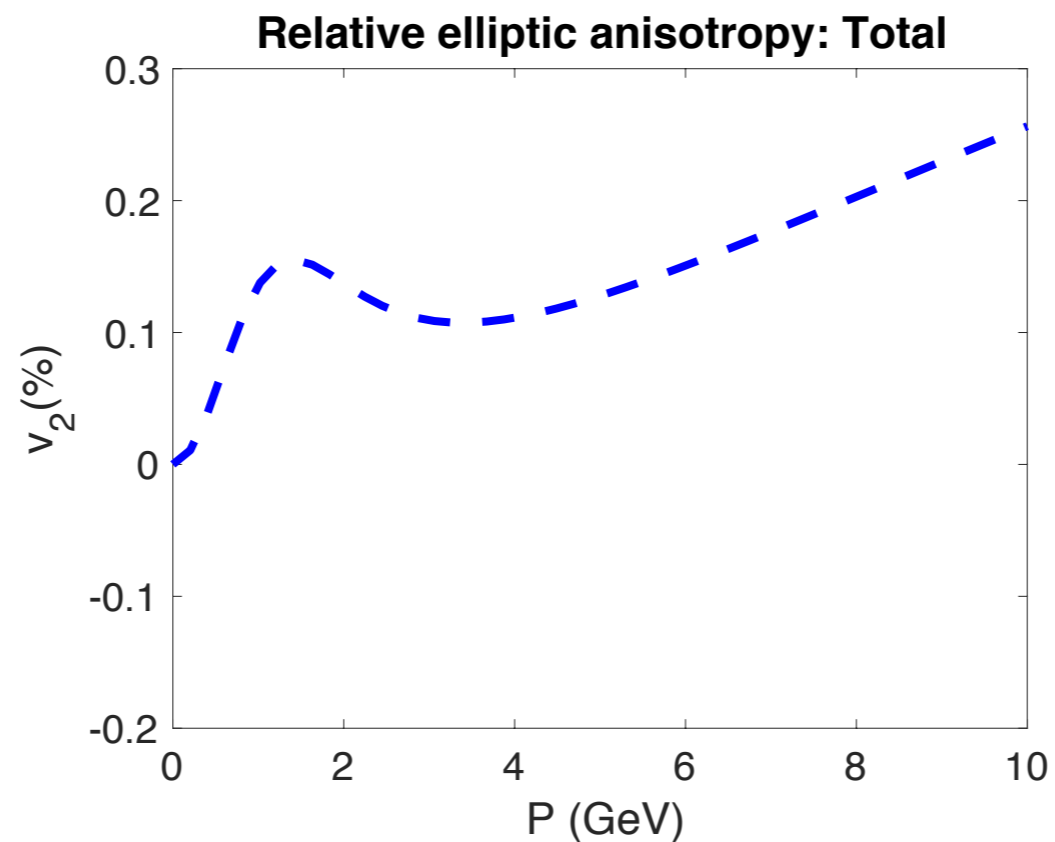
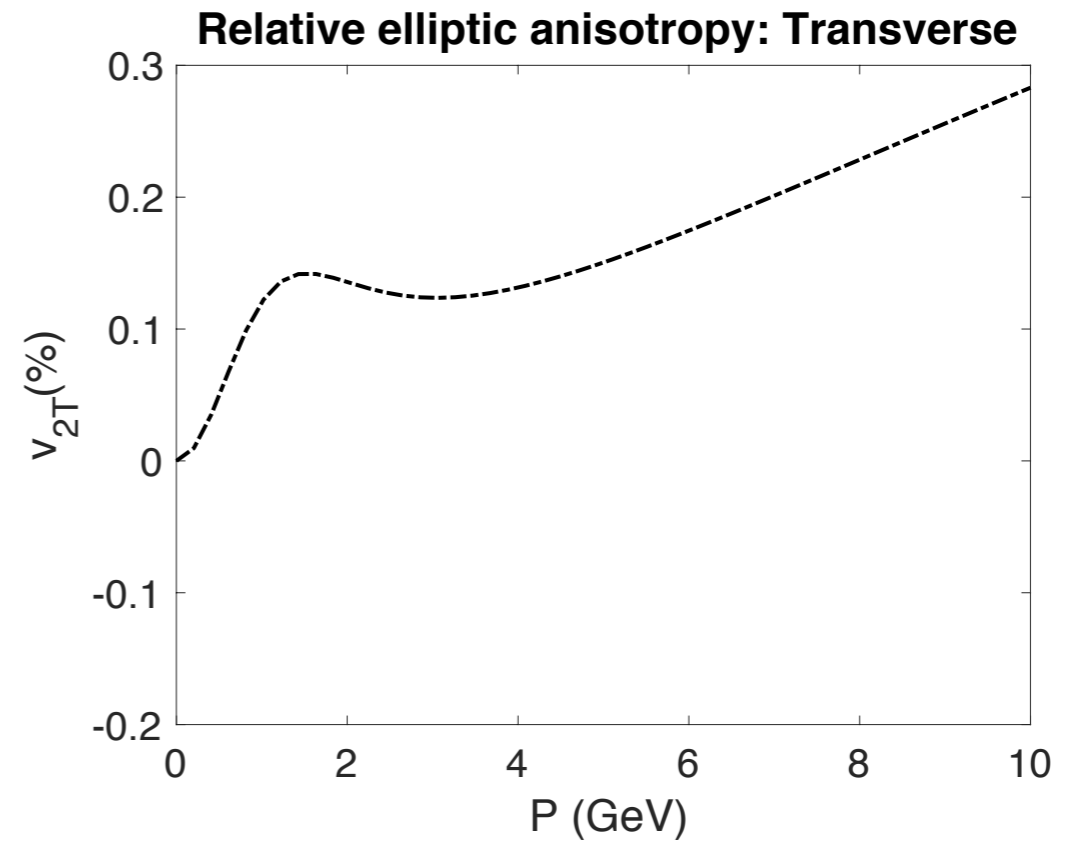
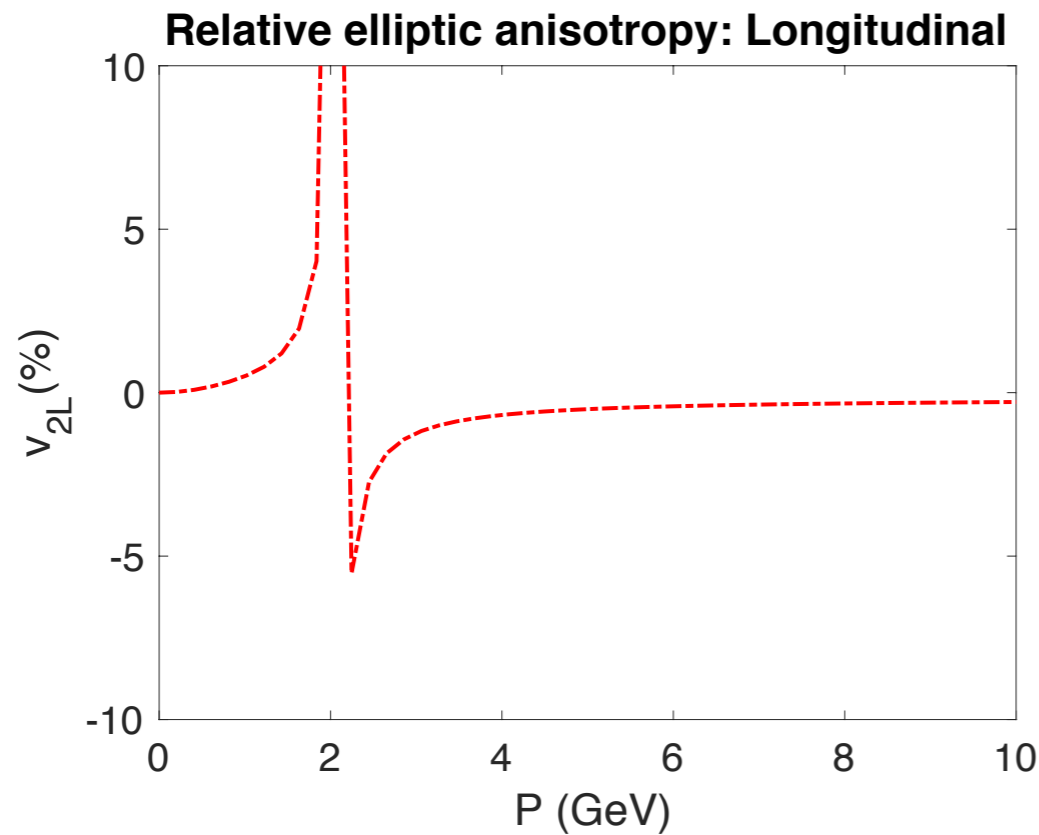
$$Q_s = 0.7 \text{ GeV}$$

$$m = 0.4 \text{ GeV}$$

$$R = 2. \text{ GeV}^{-1}$$

$$Q^2 = 1.0 \text{ GeV}$$

Semi-analytic results: Relative elliptic anisotropy (Proton)



Results are consistent with fully numerical results.

Magnitude of differential cross section, v_2 diffractive dip, etc.

Except for maximum observed at $P = 2$ GeV

Qualitative analysis

For large virtuality/massive quarks $\varepsilon_f \gtrsim Q_s^2$, one can obtain analytic expressions*.
 Example: longitudinal polarization (similar analysis for transverse):

$$\frac{d\sigma_{L,0}(P, \Delta)}{d\Omega} = \frac{8N_c\alpha_{EM}}{(2\pi)^4} Z_f^2 Q^2 z_0^3 z_1^3 Q_s^4 \frac{(P^2 - \varepsilon_f^2)^2}{(P^2 + \varepsilon_f^2)^6} |\tilde{T}(\Delta)|^2$$

dip at
 $P = \varepsilon_f$

$$\frac{d\sigma_{L,2}}{d\Omega} = \frac{8N_c\alpha_{EM}}{(2\pi)^4} z_0^3 z_1^3 Q^2 Z_f^2 Q_s^4 \frac{(\varepsilon_f^2 - P^2)P^2}{(P^2 + \varepsilon_f^2)^6} \frac{\Delta^2 |\tilde{T}(\Delta)|^2}{3m^2}$$

change in
sign in v_2

For $\varepsilon_f \approx Q_s^2$, saturation shifts the dip in P will shift to larger momentum, the scaling of cross section with Q_s saturates, among other effects.
 The P and Δ dependence does not factorize.

* We ignored the log in \mathcal{N}_0 , adding the log increases the cross section, and shifts the dip to larger P and softens the power law in P .

Conclusions/extensions

- Semi-analytic expression gives some insight into some properties of cross section and elliptic anisotropy.
- Semi-analytic expression is faster to compute than purely numerical approach. It seems to give analytic behavior and magnitude compared full numerics.
- Extend results to study semi-analytically elliptic anisotropy and cross section in inclusive dijet. Need a formula that incorporates geometry for quadrupole (Gaussian approximation?).
- Extend results to incoherent diffractive dijet. This will be sensitive to local fluctuations and gradients.

**Thanks for your
attention**